The combined measurement of ^{87}Sr/^{86}Sr isotope ratios and ^{88}Sr/^{85}Rb elemental ratios using Laser Ablation MC-ICP-MS and its application for food provenance studies: the case for Asturian beans.

Aida Reguera-Galan, Mariella Moldovan, J. Ignacio Garcia Alonso*

Department of Physical and Analytical Chemistry, University of Oviedo. Julían Clavería 8, 33006 Oviedo, Spain.

*Author to whom correspondence should be addressed:

   phone number: +34 985 10 34 84

   e-mail address: jiga@uniovi.es

ABSTRACT

The spectral interference of ^{87}Rb on ^{87}Sr for the measurement of ^{87}Sr/^{86}Sr isotope ratios in solid samples by Laser Ablation multicollector (MC)-ICP-MS could be corrected by combining the transient signal of the sample with a Rb pulse from the nebulisation of a pure Rb standard. This dual sample introduction system, combined with a multiple linear regression data treatment procedure, allowed the interference free measurement of the ^{87}Sr/^{86}Sr isotope ratio in solid samples. Additionally, when the signals for Rb and Sr could be separated in time, even only partially, the application of the multiple linear regression procedure allowed us to compute also the ^{87}Sr/^{86}Sr isotope ratio free of spectral interferences. The fact that Sr was concentrated in the seed coat of beans, whereas Rb was mainly present in the cotyledon, allowed us to develop a Laser Ablation multicollector ICP-MS procedure for the authentication of Asturian beans which are subject of fraud with the import of South American beans. By combining the ^{87}Sr/^{86}Sr isotope ratio with the ^{88}Sr/^{85}Rb elemental ratio we were able to distinguish between Asturian and South American beans in spite of the large ^{87}Sr/^{86}Sr isotopic variability of Asturian beans.

INTRODUCTION

Food traceability and the prevention of fraud in the commercialization of foodstuffs of high added value (e.g. those covered under Protected Denomination of Origin or similar legal figures) is a subject of current research interest [1]. Many analytical techniques have been proposed for food authentication purposes [2] including both molecular and elemental Mass Spectrometry techniques. Isotope ratio measurements both for the light (H, C, N, O and S) and heavy (Sr, Pb) elements have been also proposed [3, 4] and, in many cases, in combination with elemental concentrations [5,

6]. The basic idea is that the isotope ratios for the heavy elements and/or the concentration of major, minor and trace elements in plants will reflect the geology of the soil in which the plant was grown. So, for foodstuffs of plant origin, there is a direct link between the composition of the final foodstuff and the geographical coordinates of the growing soil. Unfortunately, there is not an infinite geochemical diversity in soils around the globe, and similar soil compositions and heavy element isotope ratios could be found in different soils. So, multivariate analysis is usually employed to help differentiating between geographical origins of foods and drinks of plant origin.

In this context, a few years ago we were requested by the local Asturian government to try and develop a procedure to differentiate locally grown Asturian beans (*Phaseolus vulgaris*) from beans grown elsewhere, particularly in South America. There was a lot of economic interest as the price of the local beans was ca. five times that of the South American beans. Additionally, there were suspicions that South American beans were being imported and sold as local beans. Unfortunately, those beans could not be differentiated by genetic markers so it was decided to carry out both total elemental analysis and strontium isotope ratio measurements to try and develop a method to assure the traceability of the local beans.

The measurement of $^{87}Sr/^{86}Sr$ isotope ratios in combination with elemental concentrations and multivariate data analysis is gaining acceptance and many recent publications have used this approach [7-10] for food traceability studies. The use of multicollector ICP-MS instruments is recommended for high precision strontium isotope ratios and simple quadrupole ICP-MS instruments can be applied for trace elemental analysis with satisfactory results in terms of precision and accuracy. Unfortunately, all these publications indicate that the limiting factor for the widespread use of the technique is the long and complicated sample preparation procedure, particularly for the strontium isotope ratio measurements, where the element needs to be separated from the matrix and from rubidium to avoid the isobaric interference at mass 87. These complex sample preparation procedures could be avoided if solid sampling techniques, such as Laser Ablation coupled to the ICP-MS, could be applied. So far, solid sampling techniques have never been employed in food traceability studies because of two clear limitations: first, the rubidium interference on strontium cannot be corrected easily and, second, the precision and accuracy of this technique for trace elemental analysis is still limited in comparison with solution analysis.

So, in this publication we present a novel procedure in which the spectral interference of Rb on Sr isotope ratio measurements can be corrected both for solution analysis and Laser Ablation sampling. This procedure is based on the on-line addition of a pulse of rubidium after the flow-injection or laser ablation of the sample. Then, multiple linear regression to the transient signal [11-13] is applied and the contribution of rubidium from the sample peak is automatically corrected. We have evaluated the procedure using NIST 987 strontium isotopic standard and two calcium minerals (calcite and gypsum) and finally applied it for the origin determination of Asturian beans (*Phaseolus vulgaris*). As the final procedure allows the measurement of the $^{88}Sr/^{85}Rb$ elemental ratio we have evaluated this parameter as additional discriminant with satisfactory results.

1   EXPERIMENTAL

Instrumentation

3   An Agilent 7500ce (Tokyo, Japan) ICP-MS instrument was used for multielemental
4   mapping analysis, whereas all isotope ratio measurements were conducted via a
5   Thermo Scientific Neptune Plus multicollector ICP-MS instrument (Bremen, Germany)
6   operating in low-resolution mode ($m/\Delta m=400$). A 213 nm Nd: YAG laser unit LSX-213
7   (Cetac Technologies, Omaha, USA) was coupled to both ICP-MS instruments via high-
8   purity tubing (Teflon lined Tygon tube). To enable the dual mode of sample introduction
9   for laser ablation sampling and continuous nebulisation, a Y-shaped piece was placed
10   in between the torch and the nebulisation chamber (cyclonic/double pass combined
11   spray chamber). Experimental conditions for the quadrupole and multicollector
12   instruments are given in Table 1.

Reagents and materials

14   LA-ICP-MS couplings were daily optimised using SRM NIST 612 and 610 glass
15   standards (National Institute for Standards and Technology-NIST, Gaithersburg, MD,
16   USA) for high sensitivity and low background intensity. A Rb standard from Merck
17   (Darmstadt, Germany) was used.

18   A pure crystalized calcite sample, the most common form of $CaCO_3$, was collected by
19   J.I. García Alonso. The sample of gypsum, also called *lapis specularis*, has its origin in
20   the La Condenada mine (Cuenca). Asturian, Bolivian and Argentinian beans were
21   provided by the local Asturian government.

Bean samples measured

23   Asturian beans grown under the "Protected Geographical Indication Faba Asturiana"
24   must have a minimum length of 18 mm, a maximum width of 11.5 mm and a maximum
25   thickness of 8.5 mm. Beans from 18 different locations within Asturias were measured
26   together with 2 samples from Bolivian beans and one sample from Argentinian beans.
27   All samples fitted the minimum and maximum size requirements. From each location
28   three independent beans were measured except for the South American beans where
29   five beans were measured from each location. Additionally, in each bean 9 separated
30   ablation processes were done at the top (3), center (3) and bottom (3) of the bean
31   respectively. The average of the 9 points for each bean was employed in the final
32   discrimination.

33   The map of Asturias indicating the counties where the beans were grown are shown in
34   Figure S1 in the supplementary information. Most of the samples came from the west
35   of Asturias where the main growing areas are located. The 18 samples came from
36   Vegadeo (4 producers), Tapia (1 producer), El Franco (1 producer), Coaña (1
37   producer), Tineo (1 producer), Valdés (6 producers), Ribera de Arriba (1 producer),
38   Gozón (1 producer), Siero (1 producer) and Llanes (1 producer).

Procedures

Krypton correction. The contribution of Kr impurities in the argon gas was corrected by measuring Kr at mass 83 and computing the Kr contribution ant mass 86 based on the natural Kr isotope abundances. Kr signals at mass 83 were always below 1 mV.

Multiple linear regression. The data treatment procedure is based on that published previously [13]. Basically, the time-resolved signals (S, Volts) obtained at masses 85, 86 and 87 as a function of time are treated mathematically by multiple linear regression using the function LINEST in Microsoft Excel. The signals at mass 87 are taken as "y" and the signals at masses 85 and 86 as "x". So, the time resolved data is then fitted to the equation:

$$S_{87} = a + b \times S_{86} + c \times S_{85} \tag{1}$$

Where "a" is the intercept of the regression line which corrects for background signals, "b" the isotope ratio $^{87}Sr/^{86}Sr$ and "c" the isotope ratio $^{87}Rb/^{85}Rb$. The multiple linear regression also provides the uncertainty of the different parameters (a, b and c) which can be employed for error propagation studies. 3D plots were made in MATLAB.

Mass bias correction. Mass bias correction for the $^{87}Sr/^{86}Sr$ isotope ratio measurement is usually performed internally using the $^{88}Sr/^{86}Sr$ isotope ratio as reference. This isotope ratio was calculated by standard linear regression using the signals at mass 88 as "y" and the signals at mass 86 as "x" using the function LINEST in Microsoft Excel. The time-resolved data was fitted to the equation:

$$S_{88} = d + e \times S_{86} \tag{2}$$

Where "d" is the intercept of the regression line and "e" the isotope ratio $^{88}Sr/^{86}Sr$. Finally, mass bias correction was performed using Russell's equation and the measured $^{88}Sr/^{86}Sr$ isotope ratio as reference The uncertainty of the isotope ratio $^{88}Sr/^{86}Sr$ was also computed and employed for error propagation calculations.

Error propagation.. Error propagation was performed using Kragten procedure taking into account the experimental uncertainties of the measured $^{87}Sr/^{86}Sr$ and $^{88}Sr/^{86}Sr$ isotope ratios as well as the uncertainty of the theoretical $^{88}Sr/^{86}Sr$ isotope ratio.

Computation of the Sr/Rb elemental ratio. In the Laser Ablation procedure for the origin determination of Asturian beans the Sr/Rb elemental ratio was computed as the ratio of the peak areas measured at masses 88 and 85 respectively in the transient Laser Ablation signal profile. So, the measured ratio is not really an elemental concentration ratio but rather an elemental signal ratio.

RESULTS AND DISCUSSION

Evaluation of the proposed correction procedure using Flow Injection Analysis

In our previous publication [13] the chromatographic separation of Rb and Sr was performed and the multiple regression procedure was applied to automatically correct the tailing of the rubidium peak on the strontium peak with satisfactory results. It is clear that a time separation of the strontium and rubidium signals was required for the multiple linear regression procedure to be applied. In cases where the separation of

strontium and rubidium was not possible, such as in Laser Ablation work, we believed
that a combination of two signal pulses: one for the sample, containing both Rb and Sr,
and another one for a pure Rb standard could work as an alternative to the chemical
separation of both elements. So, we prepared mixtures of NIST 987 Sr isotopic
standard with the Merck ICP-MS rubidium standard changing the concentration of
rubidium from 0:1 to 1:1 with respect to strontium and keeping the concentration of
strontium constant (400 ppb). Then we injected ca. 50 µl of this solution in a constant
flow of 2% nitric acid and after that a pure 400 ppb Rb standard. The time resolved
signal for the mixture 0.5:1 (Rb:Sr) and the subsequent injection of the Rb standard is
shown in Figure 1 while the 3D scatter plot for the signals at masses 85 (x), 86 (y) and
87 (z) is shown in Figure 2.

As it can be observed in Figure 1, two signal pulses were detected in the multicollector
instrument. The first pulse corresponded to the mixture of Rb and Sr NIST 987 while
the second pulse corresponded to the pure Rb standard. When plotting the 50 signals,
S, measured at masses 85, 86 and 87 in a three dimensional diagram (Figure 2, red
points) we get two straight lines which define a plane in the S_{85}-S_{86}-S_{87} domain. The
equation of this plane can be obtained by multiple linear regression and, in this
particular case, is equal to:

S_{87}= -0.000586 + 0.402870 x S_{85} + 0.725491 x S_{86}

Based in Figure 2, the value of 0.402870 corresponds to the slope of the plane when
S_{86}=0 and that value is the isotope ratio 87/85 for Rb. In the same way, the value of
0.725491 corresponds to the slope of the plane when S_{85}=0 and that value is the
isotope ratio 87/86 for Sr. Of course, those isotope ratios are affected by mass bias
and will need to be corrected for.

Using the same data shown in Figure 1 we can plot the signals at mass 88 vs. the
signals at mass 86 in a standard 2D x-y plot. The slope of the line obtained
corresponds to the isotope ratio 88/86 for strontium. For the particular case of the data
shown in Figure 1, this isotope ratio (R_{exp}) resulted in 8.73610. Then we applied
Russell's equation (equation 3 where m_i is the mass of ^{88}Sr and m_j the mass of ^{86}Sr) to
correct for mass bias using the theoretical value (R_{theo}) for the 88/86 isotope ratio
(8.37861) to calculate the Russell's mass bias factor , K.

$$Log\left(\frac{R_{theo}}{R_{exp}}\right) = K \times Log\left(\frac{m_i}{m_j}\right) \qquad (3)$$

Finally, the corrected 87/86 isotope ratio for strontium resulted to be 0.71049 (see
Table 2, ratio Rb:Sr 0.5:1, replicate 1) which was in agreement with the certified value
of 0.71034 within the uncertainties both of the measurements and of the certified value.

This procedure was repeated for different mixtures of Sr and Rb and the final results
are given in Table 2. As can be observed, the final corrected values for the ^{87}Sr/^{86}Sr
isotope ratio were independent of the ratio Rb:Sr. Ratios as high as 1:1 showed final
corrected ratios in agreement with the certified value. So, we can conclude that the
spectral interference of Rb on Sr can be corrected using this procedure.

Additionally, we can compare the standard uncertainties for all the experimental measurements. Both for the ratios 87/86 and 88/86 there seems to be no clear trend with the Rb:Sr ratio. So, there is not a clear increase in the experimental uncertainties with increasing Rb:Sr ratios. We have included in Table 2 also the experimental ratios measured for $^{87}Rb/^{85}Rb$. Those ratios seem to be also independent for the Rb:Sr ratio and with very low standard uncertainties.

The uncertainties for the corrected ratios given in Table 2 were calculated based on error propagation using Russell's equation. The individual uncertainties for the experimental 87/86 and 88/86 ratios as well as the standard uncertainty for the reference 88/86 ratio were combined to calculate the final total combined uncertainties shown in the last column of Table 2. The main source of uncertainty was, in all cases the uncertainty of the 88/86 reference value.

Evaluation of the proposed correction procedure using Laser Ablation sampling

As there is no solid strontium isotopic reference material available, we evaluated the procedure by analysing two high purity calcium-containing minerals (calcite and gypsum) with strontium impurities and no detectable rubidium presence. In both cases we compared the results with and without the addition of a pure rubidium pulse by nebulisation after the laser ablation sampling. The liquid carrier was 2% w/w nitric acid. To generate a transient signal for strontium, single spot ablation was selected with 0.2 mm spot size and 40 s ablation time at 20 Hz. The integration time in the MC-ICP-MS was again 4 s and 50 cycles were measured. The results obtained for a duplicate measurement of both samples are summarized in Table 3.

The main difference between both minerals was the amount of Sr present. While for the gypsum sample the signal for ^{88}Sr reached 4 V at the maximum of the LA pulse, for the calcite sample it barely reached 1 V. So, for gypsum the values and uncertainties for the corrected 87/86 ratios are very similar with and without the Rb pulse. However, for the calcite sample the uncertainties increased two-fold when Rb was nebulized after the laser ablation pulse. In conclusion, the addition of a post-laser rubidium pulse should not have any detrimental effect on the measurement of strontium isotope ratios when high enough signals are obtained for strontium. Additionally, when rubidium is present in the sample, the addition of the post-laser pulse would correct for the spectral interference of strontium.

Evaluation of strontium isotope ratios for food provenance studies using Laser Ablation sampling: the case for Asturian beans

The dissolution of the beans by high pressure digestion in a microwave oven was problematic, to say the least, and we decided to try Laser Ablation sampling. Initial studies were carried out by quadrupole ICP-MS (Agilent 7500cs). We also carried out imaging studies to elucidate in which part of the beans the elements could be concentrated. Figure 3 shows the spatial distribution of Ca, Sr, K and Rb in one of the beans measured. The photograph in the middle of the figure shows the actual half-bean analysed. The raster lines of 0.2 mm in diameter are perfectly visible. That photograph was taken a few months after the laser ablation "image" was taken and the cotyledon of the seed has shrunken noticeably (dried up).

Of interest was the fact that alkaline earth elements (Ca and Sr) were concentrated in the seed coat while alkaline elements (K and Rb) were present mainly in the cotyledon. This spatial differentiation between Rb and Sr was also observed in other seed types such as lentils and chickpeas. So, when we applied Laser Ablation sampling to the whole bean, starting from the seed coat and going into the cotyledon, this spatial separation would result in the temporal separation of the strontium and rubidium signals, i.e. we would observe first the signal from strontium in the seed coat and later on the signal for rubidium when the laser reached the cotyledon.

In fact, when we coupled the laser ablation system to the multicollector instrument we did observe this temporal separation between the strontium and rubidium signals. For example, Figure 4 shows a typical signal vs time profile for one Asturian bean after the optimisation of the measurement conditions. As it can be observed, the strontium signals appeared first while the rubidium signals appeared a few seconds later. This temporal separation of the signals allowed the application of the multiple linear regression procedure without the need for an additional rubidium pulse after the laser ablation signal simplifying in this way the analytical procedure.

To improve the separation of the strontium and rubidium signals we decided to decrease the integration time in the multicollector instrument down to 0.13 s. So, the total measurement time was ca. 60 seconds with 500 measured cycles. To improve also the separation between the Sr and Rb signals we decreased the repetition rate of the laser down to 10 Hz and the total number of bursts to 300. So, as it can be also observed in Figure 4, we measured the background both at the beginning and at the end of the peak which was ideal for successful multiple linear regression. The 3D representation of the data in Figure 4 is shown in Figure 5. In comparison with Figure 2 the data (now 500 data points) are much more scattered but still define a plane of equation:

$$S_{87} = -0.000524 + 0.401115 \times S_{85} + 0.725599 \times S_{86}$$

So, multiple linear regression can still be applied for the determination of the 87/86 Sr isotope ratio even if the temporal separation of the Sr and Rb signals is not complete.

Additionally, we observed that most of the South American beans analyzed contained a much higher concentration of strontium than the local beans. For some samples, the initial strontium peak was so high that the second rubidium peak could be seen only as a small distortion of the background. So, we decided to include a second differentiating parameter in the equation: the strontium to rubidium ratio. This was done by integrating the signals at masses 88 for strontium and 85 for rubidium and using the peak area ratio as additional discriminant. Peak area integration was done in Microsoft Excel as described previously [14].

The full data set for the measured Asturian beans is given in the Supplementary Information as Table S1. It was observed that the measurement uncertainty for each individual measurement depended drastically on the Sr/Rb elemental ratio as shown in Figure 6 for the full data set (501 individual ablation processes on 57 different beans, white points). When the $^{88}Sr/^{85}Rb$ ratio was below 0.2 the uncertainty increased

1 exponentially. Uncertainty values were below 0.001 for Sr/Rb ratios higher than 0.2,
2 with typical values of 0.0002 when the Sr/Rb ratios were higher than 2.

3 The average values and their standard deviations for each bean measured (n=9 for
4 Asturian beans or n=5 for South American beans) both for the strontium 87/86 isotope
5 ratio and for the Sr/Rb elemental ratio are shown in Table 4.

6 As it can be observed in Table 4, different beans from the same location provide very
7 similar ^{87}Sr/^{86}Sr isotope ratios except for one bean from "Coaña", marked in red, which
8 showed a very different ratio compared with the other two beans from the same
9 producer. Other minor differences between beans from the same producer were also
10 observed but, in those cases, the differences could be attributed to the low Sr/Rb ratio
11 in those particular beans which increased the uncertainties of the measurements. The
12 standard deviations of the bean averages are also plotted in Figure 6 as a function of
13 the Sr/Rb ratio (red points). As can be observed, there is a similar trend in the graph in
14 comparison with the uncertainties for each individual ablation process.

15 Finally, the average values for the ^{87}Sr/^{86}Sr isotope ratio in each bean are plotted
16 against the Sr/Rb elemental ratio in Figure 7 grouped by counties of origin. The
17 strontium isotopic signature for the Asturian beans show a large variation arising from
18 the complex geology of Asturias and the influence of sea water aerosols. Similar
19 variability results were obtained previously in the measurement of strontium isotope
20 ratios in local ciders [8]. Fortunately, the beans measured from South America show a
21 very distinct behaviour. The strontium isotope ratios for Bolivian beans are very high, of
22 the order of 0.724-0.725 which is clearly different from the Asturian beans. Additionally,
23 the Sr/Rb elemental ratio is also different, particularly for the Argentinean beans and
24 one sample from Bolivia, making the distinction between local and South American
25 beans possible. It is clear that more samples from South American beans are required
26 to confirm these results but the combination of strontium isotope ratios with strontium to
27 rubidium ratios is promising in the field of food authenticity.

28

29 CONCLUSIONS

30 We have demonstrated that the interference of Rb on Sr isotope ratios can be
31 corrected by a dual sample introduction system in which a pulse of a pure Rb standard
32 is nebulized in the MC-ICP-MS instrument after the sample pulse without a noticeable
33 increase in the uncertainty of the measurements. This procedure can be applied both
34 after nebulization of the dissolved sample or after Laser Ablation sampling. When the
35 separation in time of the Laser Ablation signals for Rb and Sr is possible, e.g. for
36 heterogeneous samples, the addition of the Rb pulse is not necessary and the multiple
37 linear regression treatment of the signals is enough to obtain the interference-free
38 ^{87}Sr/^{86}Sr isotope ratio. We have applied this procedure for the authentication of
39 Asturian beans taking advantage of the fact that strontium was present preferentially in
40 the seed coat while rubidium was found in the cotyledon. Further on, the measurement
41 of the ^{88}Sr/^{85}Rb elemental ratio served as an additional discrimination parameter as
42 South American beans showed a much higher Sr/Rb ratio than Asturian beans. Of
43 course, much more work is still necessary. The number of bean producers and
44 counties need to be increased for a complete characterisation of the "Protected

Geographical Indication Faba Asturiana" and the studies should be extended to different years and different crops. Also, we need to characterise other imported South American beans to create a complete database of foreign bean producers. At least, the procedure has been developed and seems to be working satisfactorily.

CONFLICT OF INTEREST

There are no conflicts of interest to declare.

ACKNOWLEDGEMENTS

REFERENCES

[1] L. Manning, J.M. Soon, "Developing systems to control food adulteration", Food Policy, 2014, 49, 23-32.

[2] B. Peres, N. Barlet, G. Loiseau, D. Montet, "Review of the current methods of analytical traceability allowing determination of the origin of foodstuffs". Food Control, 2017, 18, 228-235.

[3] Y. Zhao, B. Zhang, G. Chen, A. Chen, S. Yang, Z. Ye, "Recent developments in application of stable isotope analysis on agro-product authenticity and traceability". Food Chem. 2014, 145, 300–305

[4] I. Coelho, I. Castanheira, J.M. Bordado, O.F.X. Donard, J.A.L. Silva, "Recent developments and trends in the application of strontium and its isotopes in biological related fields. Trends Anal. Chem. 2017, 90, 45-61

[5] S.A. Drivelos, C.A. Georgiou, "Multi-element and multi-isotope ratio analysis to determine the geographical origin of foods in the European Union". Trends Anal. Chem. 2012, 40, 38-51.

[6] A. Gonzalvez, S. Armenta, M. de la Guardia, "Trace-element composition and stable-isotope ratio for discrimination of foods with Protected Designation of Origin", Trends Anal. Chem. 2009, 28, 1295- 1311

[7] K. Ariyama, M. Shinozaki, A. Kawasaki, "Determination of the Geographic Origin of Rice by Chemometrics with Strontium and Lead Isotope Ratios and Multielement Concentrations". J. Agric. Food Chem. 2012, 60, 1628−1634

[8] S. Garcia-Ruiz, M. Moldovan, G. Fortunato, S. Wunderli, J.I. Garcia Alonso. "Evaluation of strontium isotope abundance ratios in combination with multi-elemental analysis as a possible tool to study the geographical origin of ciders". Anal. Chim. Acta 2007, 590, 55-66

[9] M.V. Baroni, N.S. Podio, R.G. Badini, M. Inga, H.A. Ostera, M. Cagnoni, E.A. Gautier, P. Peral García, J. Hoogewerff, D.A. Wunderlin. "Linking Soil, Water, and Honey Composition To Assess the Geographical Origin of Argentinean Honey by Multielemental and Isotopic Analyses". J. Agric. Food Chem. 2015, 63, 4638−4645

[10] E. N. Epova, S. Bérail, T. Zuliani, J. Malherbe, L. Sarthou, M. Valiente, O.F.X. Donard. "$^{87}Sr/^{86}Sr$ isotope ratio and multielemental signatures as indicators of origin of European cured hams: The role of salt". Food Chem. 2018, 246, 313-322.

[11] J. Fietzke, V. Liebetrau, D. Günther, K. Gürs, K. Hametner, K. Zumholz, T.H. Hansteen and A. Eisenhauer."An alternative data acquisition and evaluation strategy for improved isotope ratio precision using LA-MC-ICP-MS applied to stable and radiogenic strontium isotopes in carbonates" J. Anal. At. Spectrom., 2008, 23, 955-961

[12] V.N. Epov, S. Berail, M. Jimenez-Moreno, V. Perrot, C. Pecheyran, D. Amouroux,. O.F.X. Donard, "Approach to measure isotopic ratios in species using MC-ICP-MS coupled with chromatography". Anal. Chem. 2010, 82, 5652–5662.

[13] J.A. Rodríguez Castrillón, S. García Ruiz, M. Moldovan, J.I. García Alonso. "Multiple Linear Regression And On-Line Ion Exchange Chromatography For Alternative Rb-Sr And Nd-Sm MC-ICP-MS Isotopic Measurements". J. Anal. At. Spectrom., 2012, 27, 611-618.

[14] S. Queipo Abad, P. Rodriguez-Gonzalez, J.I. Garcia Alonso. "Evidence of the direct adsorption of mercury in human hair during occupational exposure to mercury vapour". J. Trace El. Med. Biol., 2016, 36, 16-21

1

Table 1. Experimental conditions

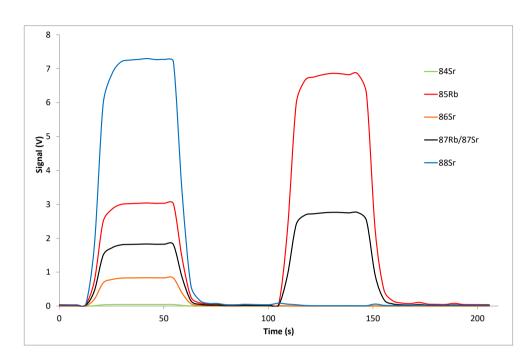| Multielemental analysis						
Q-ICP-MS instrumental and acquisition parameters						
RF Power (W)	1500					
Ar plasma gas flow (L min^{-1})	15					
Ar carrier gas flow (L min^{-1})	0.75					
Acquisition mode	Time resolved analysis					
Points per peak	1					
Integration time per point (s)	0.1					
Monitored mases	^{39}K, ^{43}Ca, ^{85}Rb, ^{88}Sr					
Laser ablation instrumental parameters						
Laser energy output	100% (5.6 mJ max)					
Repetition rate (Hz)	20					
Spot size (µm)	200					
Distance between lines (µm)	200					
Scan rate (µm s^{-1})	10					
Isotope Ratio measurement						
MC-ICP-MS instrumental and acquisition parameters						
RF Power (W)	1200					
Ar plasma gas flow (L min^{-1})	15					
Ar carrier gas flow (L min^{-1})	0.70					
Ar auxiliary gas flow (L min^{-1})	0.50					
Integration time (s)						
- nebulised solution	4.20					
- laser ablation	4.20 – minerals					
	0.13 - beans					
Number of blocks	1					
Number of cycles	50 – nebulised solution and minerals					
	500 - beans					
Resolution	Low					
Mode	Static					
MC-ICP-MS Cup configuration						
L3	L2	L1	C	H1	H2	H3
^{82}Kr$^+$	^{83}Kr$^+$	^{84}Sr$^+$	^{85}Rb$^+$	^{86}Sr$^+$	^{87}Sr$^+$	^{88}Sr$^+$
		^{84}Kr$^+$		^{86}Kr$^+$	^{87}Rb$^+$	
Laser ablation instrumental parameters						
Laser energy output	100% (5.6 mJ max)					
Repetition rate (Hz)	20 – minerals					
	10 - beans					
Spot size (µm)	200					
Bursts	800 – minerals					
	300 - beans					
Helium flow (L min^{-1})	0.45					

3

1

2

3

Figure 1. Time-resolved signal for the mixture of Rb and Sr NIST 987 (0.5:1) and the
pure Rb standard (50 data points, 4 s integration time).

6

1

2

3   **Figure 2**. 3D scatter plot of the signal at mass 87 vs. the signals at masses 85 and 86
4   for the data in Figure 2. The grid shown is the plane that best fits the data points by
5   multiple linear regression (S_{87}= -0.000586 + 0.402870 x S_{85} + 0.725491 x S_{86}).

Table 2. Correction of the rubidium spectral interference on strontium by multiple linear regression and Flow Injection Analysis

Ratio Rb:Sr	Replicate	R_{Exp} (87/86)	u_{Exp}(87/86)	R_{Exp} (88/86)	u_{Exp}(88/86)	R_{Exp} (87/85)	u_{Exp}(87/85)	R_{Cor} (87/86)	u_{Cor}(87/86)
0:1	1	0.725578	0.000033	8.73740	0.00030	0.402914	0.000005	0.71044	0.00008
	2	0.725530	0.000035	8.73695	0.00019	0.402900	0.000005	0.71041	0.00008
0.01:1	1	0.725452	0.000046	8.73589	0.00021	0.402867	0.000006	0.71038	0.00008
	2	0.725499	0.000032	8.73609	0.00024	0.402858	0.000004	0.71041	0.00008
0.1:1	1	0.725483	0.000028	8.73604	0.00025	0.402851	0.000004	0.71040	0.00008
	2	0.725514	0.000041	8.73625	0.00023	0.402859	0.000005	0.71042	0.00008
0.33:1	1	0.725511	0.000035	8.73698	0.00026	0.402887	0.000005	0.71039	0.00008
	2	0.725491	0.000049	8.73683	0.00024	0.402870	0.000007	0.71038	0.00008
0.5:1	1	0.725573	0.000034	8.73610	0.00030	0.402855	0.000004	0.71049	0.00008
	2	0.725541	0.000041	8.73610	0.00029	0.402861	0.000005	0.71046	0.00008
1:1	1	0.725447	0.000049	8.73585	0.00025	0.402870	0.000005	0.71037	0.00008
	2	0.725453	0.000055	8.73647	0.00027	0.402870	0.000006	0.71035	0.00009
Mean*								**0.71041**	**0.00016**
Reference**				**8.37861**	**0.00325**			**0.71034**	**0.00026**

*Average of the 12 independent values and expanded uncertainty at the 95% level by combining the standard error of the 12 measurements and the standard uncertainty for each independent measurement.

**Uncertainties in the reference material are indicated as expanded uncertainties at the 95% confidence level. For error propagation those expanded uncertainties have been divided by a coverage factor of 2 to calculate the standard uncertainties.

Table 3. Evaluation of the post-laser rubidium pulse

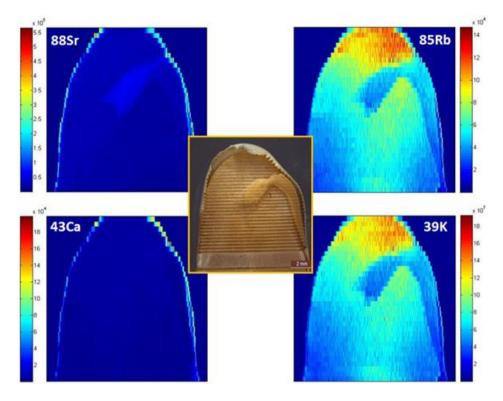| Mineral	Without Rb-pulse		With Rb-pulse	
	$R_{Cor}(87/86)$	$u_{Cor}(87/86)$	$R_{Cor}(87/86)$	$u_{Cor}(87/86)$
Calcite (1)	0.70912	0.00020	0.70880	0.00042
Calcite (2)	0.70886	0.00023	0.70894	0.00043
Gypsum (1)	0.70781	0.00014	0.70786	0.00016
Gypsum (2)	0.70782	0.00015	0.70790	0.00016

Figure 3. Spatial distribution of Ca, Sr, K and Rb in the seeds.
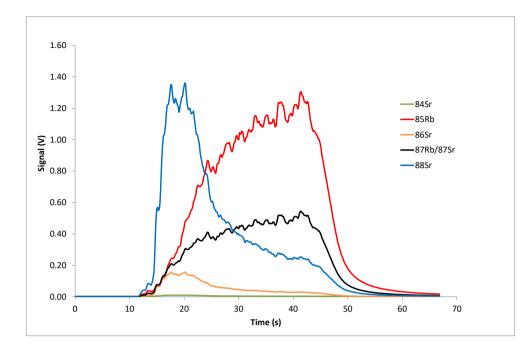
Figure 4. Signal vs time profile for the laser ablation sampling (single spot ablation) of one Asturian bean from Vegadeo.
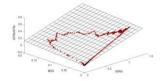
Figure 5. 3D scatter plot of the signal at mass 87 vs. the signals at masses 85 and 86 for the data in Figure 4. The grid shown is the plane that best fits the data points by multiple linear regression ($S_{87} = -0.000524 + 0.401115 \times S_{85} + 0.725599 \times S_{86}$).
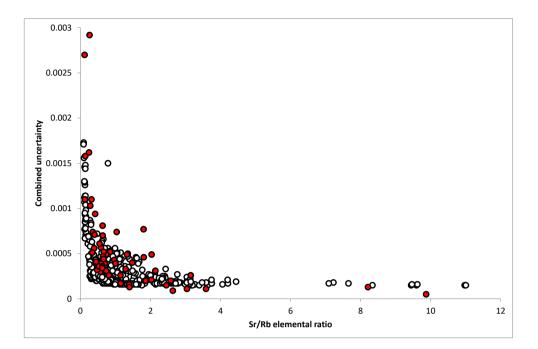
Figure 6. Combined uncertainties for each individual 87/86 isotope ratio as a function of the Sr/Rb elemental ratio (501 ablation processes on 57 different beans, white points) and standard deviation for the bean averages (red points).

Table 4. Individual average and standard deviation results (per bean) for the ^{87}Sr/^{86}Sr isotope ratio and the ^{88}Sr/^{85}Rb elemental ratio.

Origin	Bean sample	^{87}Sr/^{86}Sr	Std. dev.	^{88}Sr/^{85}Rb	Std. Dev.
Ribera	1a	0.71352	0.00074	0.348	0.046
	1b	0.71338	0.00026	0.812	0.099
	1c	0.71359	0.00041	0.633	0.148
Llanes	2a	0.70821	0.00011	3.040	0.343
	2b	0.70879	0.00015	2.449	0.307
	2c	0.70891	0.00033	1.288	0.061
Valdes (1)	3a	0.70926	0.00043	0.963	0.125
	3b	0.70952	0.00031	0.605	0.047
	3c	0.70926	0.00017	1.151	0.099
Vegadeo (1)	4a	0.71076	0.00057	0.581	0.090
	4b	0.71136	0.00030	0.570	0.083
	4c	0.71164	0.00031	0.731	0.108
Vegadeo (2)	5a	0.71132	0.00158	0.134	0.017
	5b	0.71168	0.00039	0.691	0.114
	5c	0.71028	0.00162	0.242	0.070
Siero	6a	0.71014	0.00049	1.326	0.158
	6b	0.71011	0.00052	0.848	0.126
	6c	0.71034	0.00046	1.807	0.401
Coaña	7a	0.70701	0.00021	2.023	0.327
	7b	0.70675	0.00011	3.582	0.398
	7c	0.71100	0.00049	2.030	0.442
Valdes (2)	8a	0.71031	0.00071	0.398	0.062
	8b	0.70928	0.00292	0.258	0.063
	8c	0.71012	0.00094	0.417	0.067
Gozon	9a	0.71057	0.00039	0.997	0.153
	9b	0.71010	0.00026	3.146	0.821
	9c	0.70987	0.00031	2.136	0.149
Vegadeo (3)	10a	0.71054	0.00020	2.576	0.443
	10b	0.71066	0.00009	2.634	0.167
	10c	0.71044	0.00020	1.858	0.502
Valdes (3)	11a	0.71132	0.00110	0.311	0.042
	11b	0.71162	0.00056	0.388	0.078
	11c	0.71161	0.00103	0.278	0.026
Valdes (4)	12a	0.71329	0.00110	0.128	0.008
	12b	0.71064	0.00039	0.577	0.123
	12c	0.71058	0.00041	0.444	0.052
Vegadeo (4)	13a	0.71196	0.00032	0.475	0.078
	13b	0.71129	0.00077	1.800	0.585
	13c	0.71081	0.00070	0.632	0.074
Tineo	14a	0.71238	0.00040	1.475	0.378
	14b	0.71251	0.00081	0.629	0.045

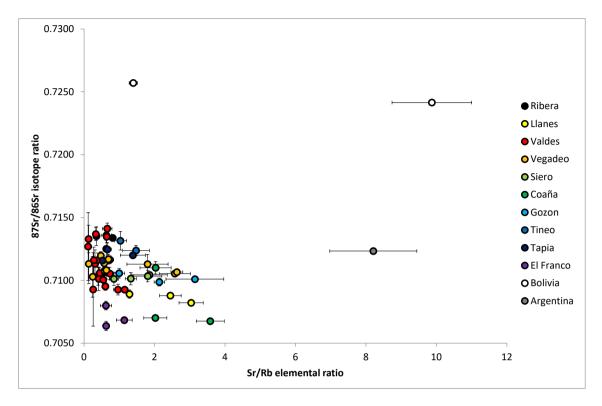|					
	14c	0.71315	0.00074	1.031	0.174
Valdes (5)	15a	0.71005	0.00061	0.542	0.043
	15b	0.71055	0.00049	0.729	0.087
	15c	0.71269	0.00270	0.116	0.026
Tapia	16a	0.71246	0.00052	0.661	0.115
	16b	0.71200	0.00016	1.387	0.356
	16c	0.71158	0.00036	0.525	0.034
El Franco	17a	0.70684	0.00026	1.142	0.223
	17b	0.70638	0.00036	0.626	0.066
	17c	0.70799	0.00034	0.621	0.160
Valdes (6)	18a	0.71368	0.00051	0.334	0.068
	18b	0.71348	0.00047	0.640	0.086
	18c	0.71411	0.00044	0.658	0.135
Bolivia	19	0.72415	0.00005	9.869	1.130
	20	0.72571	0.00013	1.398	0.118
Argentina	21	0.71233	0.00013	8.209	1.236

Figure 7. Discrimination between Asturian and South American beans based on the $^{87}Sr/^{86}Sr$ isotope ratio and the $^{88}Sr/^{85}Rb$ elemental ratio. Error bars correspond to the standard deviation for n=9 (Asturian beans) or n=5 (South American beans) measurements.